# Charge transfer and superconductor-metal-insulator transitions in high-$T_c$ superconductors

J. C. Phillips
*AT&T Bell Laboratories, Murray Hill, New Jersey 07974*
(Received 21 July 1994)

We propose a microscopic model for the large double-layer capacitance and resistance jumps $\Delta C_{DL}$ and $\Delta R_{DL}$ which occur at $T=T_c=112$ K at the interface between the cuprate superconductor $Tl_{2223}$ and an organic liquid electrolyte, as measured by Peck *et al.* The jumps are associated with changes in the superconductor-metal-insulator micromorphology of Josephson junctions which are weak links in the Tinkham-Blackstead network model of the high-temperature superconductive transition. Ion-channeling experiments strongly support the model explanation for the 10–30 % effects which are seen over $\Delta T \lesssim 0.5$ K.

One of the most popular ideas for describing chemical trends in the superconductive properties of high-temperature superconductors (HTS's) is that of charge transfer. For materials with $T_c \sim 100$ K, such as Y-Ba-Cu-$O_{6+x}$, the bismates, thallates, and mercurates, charge transfer is supposed to occur between $CuO_2$ planes and suitable metallic charge reservoirs placed midway between these planes. (These reservoirs would be the $CuO_x$ chains in Y-Ba-Cu-$O_{6+x}$, or the bismate, thallate, or mercurate planes in the other materials.) One formulation[1,2] of this idea for Y-Ba-Cu-$O_{6+x}$ has been cited in some 600 papers. Our own view[3] of this situation is that the mechanism responsible for high $T_c$'s in these cuprates is considerably more complex, but that charge transfer, although far from being the whole story (size effects and layer buckling are equally important), plays a very important role. This being the case, experiments which measure charge transfer directly, and which exhibit a large effect at $T=T_c$, are of great interest.

Such experiments have been carried out by measuring the frequency dependence of the double-layer capacitance and resistance of electrolyte/HTS interfaces.[4,5] [Physicists who are not familiar with experiments of this type may wish to compare the methods and results of the low-temperature experiments discussed here with room-temperature electroreflectance (optical modulation) spectroscopy of semiconductors.[6]] The electrolyte may be either solid[4] or liquid,[5] but by far the most reproducible and largest effects are obtained with a carefully selected organic electrolyte eutectic solution[7] which retains a high ionic conductivity at temperatures down to 88 K and which is nondestructive. It is likely that contact between the solid electrolyte and the HTS occurs at isolated points, and that most of these contacts damage the HTS substrate, and locally reduce $T_c$, greatly reducing the magnitude of the observed effects.

For the reader's convenience we reproduce in Fig. 1 the Nyquist impedance plots of a liquid electrolyte-$Tl_{2223}$ electrode interface. The frequency range varies from $10^4$ to $10^{-2}$ Hz from left to right. The curves are the combination of three arcs of increasing magnitude from left to right. By varying bias voltage it was shown[5] (again from left to right) that the arcs represent a stray circuit impedance, the electrolyte impedance, and the double-layer interfacial impedance. Each impedance $Z(\omega)$ is represented by

$$Z(\omega)=R/[1+jRC(j\omega)\omega]\,, \tag{1}$$

$$C(\omega)=C_0(\omega/\omega_0)^{-\delta}\,, \tag{2}$$

where $\delta$ is a nonideality factor. In practice $\delta \sim 0.2$–$0.4$ and its nonzero value can be understood[8] as the result of inhomogeneities which give rise to the Tinkham-Blackstead network[9,10] which is an essential element of our multiphase superconductor-metal-insulator model discussed below.

Again, for the reader's convenience, we reproduce in Fig. 2 the measured values of the double-layer capacitance $C_{DL}(T)$ for several bias voltages. The figure also shows a similar plot for a glassy carbon electrode. It is found that $C_{DL}(T)$ decreases by 10–30 % over a $\Delta T$ in-

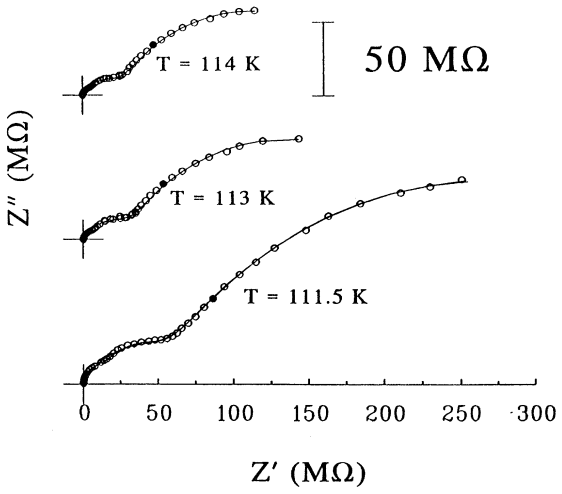


FIG. 1. Nyquist impedance plots (crosses denote origins) for a $Tl_{2223}$ ($T_c=112$ K) electrode. Reprinted with permission from Ref. 5. Copyright 1992 American Chemical Society.

 

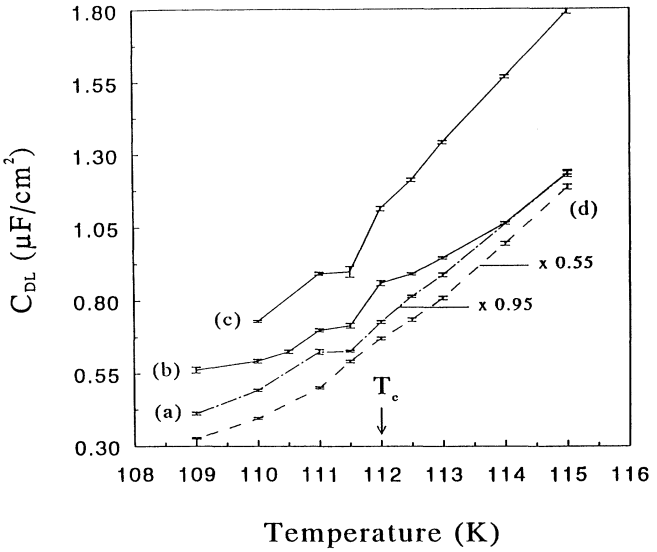


FIG. 2. Steps in $C_{DL}(T)$ obtained from data of the kind shown in Fig. 1. Curve $d$ is a glassy carbon electrode, while curves (a)–(c) are obtained from the low-frequency arcs in Fig. 1. Reprinted with permission from Ref. 5. Copyright 1992 American Chemical Society.

terval of 0.5 K centered on $T_c$ ($Tl_{2223}$). This is a very large effect, and it is surprising for at least three reasons: (1) For a metallic electrode the electrode contribution to the double-layer capacitance should be small compared to that of the electrolyte, because the metallic plasma screening length is $\lesssim 1$ Å, compared to the electrolyte Debye screening length of order 5 Å or more. (2) The metallic screening length is in any event virtually unchanged by the normal-superconducting transition. This is because the superconductive energy gap $E_g$ is of order 0.05 eV, while the metallic plasma energy $\hbar\omega_p$ is of order 10 eV. (3) The normal-superconductive transition is supposed to be second order, but the large effects shown in Fig. 2 are clearly first-order discontinuities in $C(T)$, not discontinuities in $dC(T)/dT$.

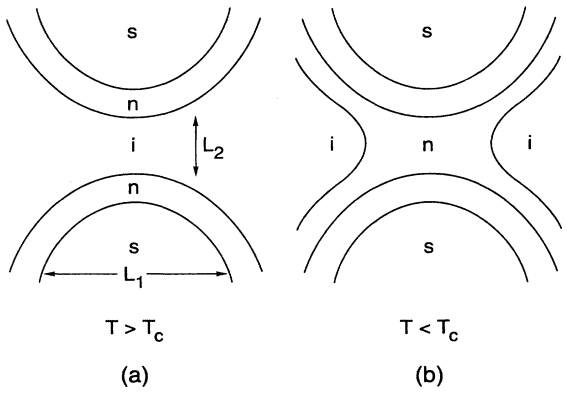


FIG. 3. Saddle-point nanojunctions [$s$-$n$-$i$-$n$-$s$ for $T > T_c$ in (a), $s$-$n$-$s$ for $T < T_c$] in a plan view of the HTS electrode layer. The dimensions are $L_1 \sim 100$ Å and $L_2 \sim 20$ Å.

We now develop a microscopic model which resolves these difficulties. As we have stressed for some time,[11] the micromorphology of oxide HTS's must be very different from that of intermetallic superconductors such as Pb or $Nb_3Sn$, as HTS materials are structurally and chemically[12] closely related to perovskite ferroelectrics, which exhibit a variety of domain and other inhomogeneous effects of a ferroelectric nature. As a result of these inhomogeneities on a scale small compared to the penetration depth superconductivity actually occurs in discrete regions connected by weak links which can be regarded in some respects as Josephson junctions. This description gives a very accurate account[11,12] not only of the resistivity $\rho(T,H)$ transitions near $T_c$ in granular samples, but even in the best available single crystals[13] of Y-Ba-Cu-O ($\Delta T_c \sim 0.1$ K).

Given the great success of the Tinkham-Blackstead model, what is the proper description of the microstructure of the Josephson weak links? We can explain the charge-transfer data shown in Figs. 1 and 2 if we assume that this microstructure has the three-phase form shown in plan view of the HTS electrode surface in Fig. 3, and that the superconductive normal metallic, and insulating regions are all graded continuously with respect to a single microscopic parameter, which we denote by $X$. The nature of this parameter $X$ will be discussed below, but first let us see how the three-phase weak-link model shown in Fig. 3 explains the large steps shown in Fig. 2.

In Fig. 3(a) we show the weak link for $T > T_c$. The junction is an $s$-$n$-$i$-$n$-$s$ junction between isolated precursive superconductive patches whose dimensions $L_1$ are of order 100 Å or less, that is, much less than the London penetration depth $\lambda \gtrsim 1000$ Å. The Meissner screening currents associated with such patches are negligible, because magnetic flux lines easily bypass these regions and there is no magnetic-field expulsion. The coupling between superconductive regions is negligible because the dimension $L_2$ of the insulating barriers is of order 20–30 Å.

A percolative superconductive transition occurs at $T = T_c$. The suerconductive regions expand as $X$ increases with decreasing $T$, and as they expand the $i$ junction region is squeezed out, so that a critical percolative fraction of weak links is now $s$-$n$-$s$. The change from (a) to (b) has two effects. The first, the establishment of bulk superconductivity, occurs because the $s$-$n$-$s$ links establish superconductive phase coherence on a scale large compared to $\lambda$. The second effect is that in (a) the $i$ regions were connected, but now in (b) the $n$-$s$ regions are connected. The $i$ regions make a substantial contribution to $C_{DL}$ when they are connected (a), but this contribution is screened in (b) by image charges in the connected $n$-$s$ regions. This explains why there is a large change in $C_{DL}$ at $T = T_c$. The same change in weak-link topology which produces the metal-superconductor percolative phase transition also produces a metal-insulator charge-transfer screening transition.

This point can be developed further in the context of an effective-medium model for the temperature dependence of the frequency- and wave-number-dependent

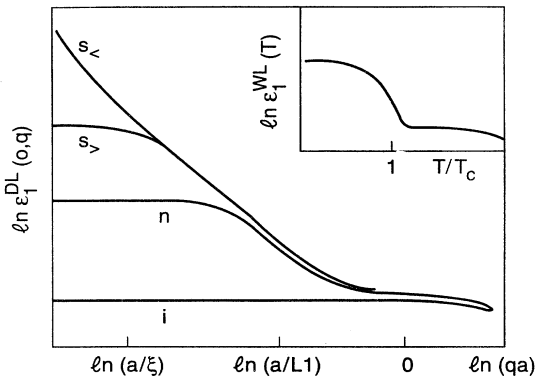


FIG. 4. The effective-medium dielectric constant $e_1^m(0,q)$ has three contributions, corresponding to an insulator $i$, a normal metal $m$, and a superconductor ($s_>$, $T>T_c$, and $s_<$, $T<T_c$). The final value for $\varepsilon_1^{WL}(T)$ shown in the inset is a suitably weighted average of these contributions, which varies rapidly as $T$ goes through $T_c$, as shown in the inset.

effective dielectric constant $\varepsilon_1^{WL}(\omega,q,T)$ of the three-phase weak-link region, as shown in Fig. 4. Each phase is represented by a spheroid of diameter $L_1$ (insulating and metallic phases) or $\xi$ (superconductive phase), where we assume $\xi > L_1$. [In fact, the effective coherence length at $T=T_c$, $\xi(T_c)$, will be cut off at a value somewhat larger than $L_1$, but not infinite, as in an infinite superconductive medium.] For a given three-phase geometry, such as that illustrated in Figs. 3(a) and 3(b), the effective-medium dielectric approximation to the weak-link constant $\varepsilon_1^{WL}(T)$ will be a weighted average over $q$, with weighting functions $w_i(q)$, $w_m(q)$, and $w_s(q)$ for the three microphases, which depend on the geometry. However, for $q(L_1$ or $\xi) \lesssim 1$ the largest weight will be given to the connected phase. Thus for these long-wavelength $q$ we have for $T_> = T > T_c$ (where only the insulating phase is connected) a greater weight for $w_i(q)$, and $\varepsilon_1^{WL}(T_>)$ will be close to $\varepsilon_1$ (insulator). However, for $T<T_c$, greater weight will be given to the metallic and superconductive weighting functions, and $\varepsilon_1^{WL}(T_<)$ will be closer to $\varepsilon_1$ (metal) and $\varepsilon_1$ (super). Thus there will be a jump in the double-layer impedance $Z_{DL}(T)$ at $T=T_c$, as shown in Fig. 4.

There is additional information in the model besides this jump. Most of the difference between $\varepsilon_m(q)$ and $\varepsilon_i(q)$ occurs at small $q$ and $q \sim \omega v_F$, where $v_F$ is the Fermi velocity in the metal. (We assume that the mean free path $l$ in the metal satisfies $l \gtrsim L_1$.) Thus most of the jump in $Z(\omega)$ occurs in $C_{DL}$, and if $l \gg L_1$, the jump $\Delta R_{DL}$ would be much less than $\Delta C_{DL}$. In fact, however, $l$ is still $\sim L_1$, so there are jumps $\Delta R_{DL}$ as well. However, these are expected to be smaller and less reproducible (more dependent on network geometry) than $\Delta C_{DL}$, as observed experimentally.[5]

The functional form of the jump or analytic singularity in the weighting functions $w_\alpha(q,T)$ depends on how the geometry of the image charges is affected by the changes in connectivity at $T=T_c$. We will not attempt a full treatment of this effect here, but we can note that the saddle-point geometry shown in Fig. 3 is highly suggestive as regards such analytic singularities. The number of long-wavelength ($q<q_c$) insulating image charge Fourier components should increase like $(T-T_c)^{1/2}$ for $T>T_c$, because $X(T)$ varies linearly with $T$, and near the saddle point where $X=X_c$, the energy difference $\Delta E_{im}$ between insulating and metallic phase should vary quadratically with $X$. The same square-root singularity occurs in the relative volumes of the metallic and insulating regions as $T$ passes through $T_c$; it is a characteristic feature of networks of saddle points.[14]

We must now explain the microscopic meaning of the grading parameter $X$. We believe that this parameter essentially measures the contribution to $n(E_F)$, the density of electronic states at the Fermi energy, associated with resonant pinning states derived from oxygen vacancies or interstitials in regions where the layer buckling is small. The applied dc bias voltage and the modulation voltage are both of order 1 V, and as much as 0.1 V may be available to displace HTS oxygen atoms from one configuration to another. In fact, if such displacements change substantially at $T=T_c$, then they should be observable experimentally. We would not expect, however, to be able to observe them by diffraction, because diffraction averages such displacements over the entire sample, whereas we are concerned with reconstruction of oxygen resonant pinning centers only in the weak links. An experimental technique which is sensitive to a small fraction of athermally large atomic displacements is ion channeling. The results[15] for the effective Debye-Waller

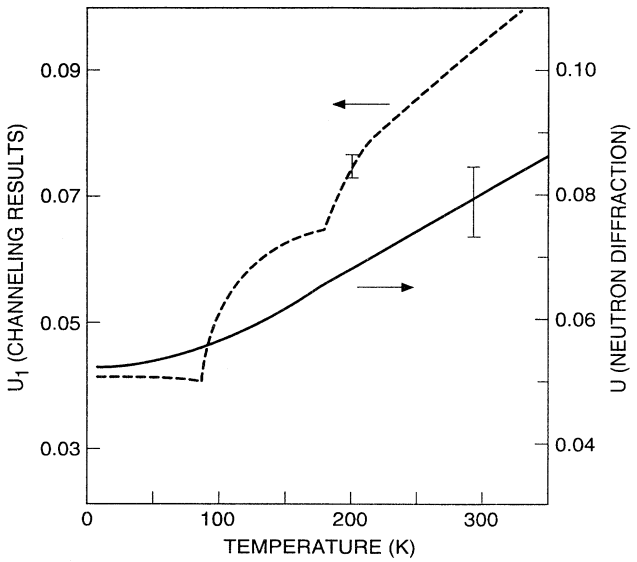


FIG. 5. The effective Debye-Waller factor displacement $U_1$ measured by ion channeling, compared with the actual value $U$ measured by neutron diffraction, in Y-Ba-Cu-O [see Ref. 14 and J. C. Phillips, in *Lattice Effects in High-$T_c$ Superconductors*, edited by Y. Bar-Yam, T. Egami, J. Mustre-de Leon, and A. R. Bishop (World Scientific, Singapore, 1992), p. 3].

displacement $\overline{u^2}$ measured by this method are shown in Fig. 5, again for the reader's convenience, against true Debye-Waller displacements obtained by neutron diffraction in Y-Ba-Cu-O as a function of temperature. The magnitude of the ion-channeling jump in $\overline{u^2}$ near $T_c$ is of order 30%, which is quite comparable to the jump in $C_{\rm DL}$ shown in Fig. 2. In other words, we have in Fig. 5 independent evidence for substantial reconstructive displacements of oxygen atoms in small regions, as required so that Fig. 3 can explain Fig. 2. The data are even consistent with the $(T-T_c)^{1/2}$ saddle-point behavior mentioned above.

The smooth line drawn through the data in Fig. 5 corresponds to a very narrow second-order phase transition, which is not easily distinguished experimentally from a first-order phase transition. The range $L_2$ of forces associated with this transition would then be much larger than that associated with a BCS transition at $T_c$. Such a large $L_2 \gg L_1$ could be the result of ferroelastic strain forces, because in perovskite structures such forces often produce domain sizes of order $1\mu$ (ferroelectric domain dimensions).

We can discuss the magnitude of the voltages which affect these atomic displacements $X$. The latter can alter the superconductive boundary regions because they displace peaks in the density of states $N(E)$ which is represented by[3]

$$N(E)=N_b(E)+N_r(E,X)\ , \tag{3}$$

where $N_b(E)$ is the band density of states and $N_r(E,X)$ represents a dopant contribution of resonant pinning states peaked at $E=E_0(X)$, where $E_0(X)$ is close to $E_F$. There is already evidence in layered tellurides and sulfides which suggests that as $T$ decreases $E_0 \rightarrow E_F$ (the anti–Jahn-Teller effect).[16] The activation energy obtained in internal friction measurements[3,17] for these $X$ displacements is $E_A \sim 0.16$ eV. We note that this energy is comparable to the fraction 0.1 V of the applied and modulation voltages ($\sim 1$ V) which can be expected to apply to a single unit cell in a rough surface layer $\sim 50$ Å thick. Thus the strength of the coupling of the external field to internal displacements of resonant pinning centers which contribute to $C_{\rm DL}$ is reasonable.

We mention here another experiment[18] on surface charging in which the work function (or chemical potential) $\mu(T)$ of laser-ablated Y-Ba-Cu-$O_{6+x}$ films was measured as a function of temperature through $T_c$. Below $T_c$ the data show a rapid increase in $\mu_s(T)$ relative to the extrapolated value of $\mu_n(T)$. These data were interpreted in the context of homogeneous metallic surface states.[18] However, we have grave doubts concerning the applicability of this model. We have remarked elsewhere[3] that such laser-ablated films show phonon structure in their far-infrared reflectivity which corresponds predominantly to bulk phonon energies, measured independently by neutron scattering, associated with the insulating phase, $x \lesssim 0.3$, not the metallic $T_c \sim 90$ K phase, $x \sim 0.9$. This is consistent with a filamentary surface Tinkham-Blackstead network, not a homogeneously metallic surface. Then the measured chemical potential $\mu(T)$ will depend in a complex way on the differences between $\mu_i$, $\mu_n$, and $\mu_s$, with appropriate temperature-dependent weighting factors. In the double-layer experiments[5] discussed here, the same weighting problem arises as well. Again in the work function measurements[18] an anomalously large effect was found which was ascribed to two-dimensional surface superconductivity.[18] We believe that this large effect, with $d\mu/dT$ changing discontinuously at $T=T_c$, is the result of competing filling factors for the insulating, metallic, and superconductive microphases which coexist at the sample surface, and does not measure the density $n$ of surface charge carriers. Instead it reflects spinodal changes of a few percent or less in the insulating filling factor below $T_c$; changes of this order of magnitude are what one expects from Fig. 3 of the present paper with $L_2 \sim 10^{-1} L_1$.

Another question which can be raised is how the screening charge depends on the nature and density of the defects which generate the weak links. This is a difficult question to answer because we know so little about the latter. Similar questions arise in connection with vortex pinning, and there so far we have information largely on qualitative trends from one material to another. For example, in $YBa_2Cu_3O_{6.9}$ ($T_c \sim 90$ K) samples vortex pinning appears to be dominated by point defects,[10,19] but stacking faults and edge dislocations seem to be more important[10] in $Bi_2Sr_2CaCu_2O_{8+\delta}$. Extended defects may produce larger values of $\Delta Z_{\rm DL}/Z_{\rm DL}$ than point defects, and if we assume that $Tl_{2223}$ is similar to $Bi_{2212}$, then this would suggest that the already studied $Tl_{2223}$ has larger $\Delta Z_{\rm DL}/Z_{\rm DL}$ than $Y_{1237}$ has. The latter also lies at the edge of the temperature range accessible to the electrolyte technique. As for the Hg cuprates, with $T_c \sim 130$ K, it seems likely that these also have fewer extended defects.[20]

In conclusion, we have explained the very large charge-transfer effects obtained experimentally at $T=T_c$ in terms of a superconductive-metal-insulator model of the micromorphology of superconductive weak links in a percolative network model. Inasmuch as these weak links determine the superconductive transition, we believe that this model is the most realistic one proposed to date to explain the microscopic nature of the superconductive transition in HTS's. An idealized homogeneous model of interlayer capacitance Josephson junctions for the cuprates, in which the spatially localized Tinkham-Blackstead junctions are extended across entire $CuO_2$ layers, has been discussed elsewhere.[21]

I am grateful to Dr. B. Batlogg for drawing my attention to Ref. 18.

[1]R. J. Cava *et al.*, Nature **332**, 814 (1988).
[2]R. J. Cava *et al.*, Physica C **165**, 419 (1990).
[3]J. C. Phillips, Physica C **221**, 327 (1994); Phys. Rev. Lett. **72**, 3863 (1994).
[4]M. W. Breitner, W. J. Lorenz, and G. Sacmann-Ischenko, Surf. Sci. **230**, 213 (1990); A. Pinkowski *et al.*, Europhys. Lett. **9**, 269 (1989).
[5]S. R. Peck *et al.*, J. Am. Chem. Soc. **114**, 6771 (1992).
[6]M. Cardona, Solid State Phys. Suppl. **11**, 1 (1969).
[7]J. T. McDevitt, D. R. Riley, and S. G. Haupt, Anal. Chem. **65**, 535A (1993).
[8]J. C. Dyre, Phys. Rev. B **47**, 9128 (1993); **48**, 12 511 (1993).
[9]M. Tinkham, Phys. Rev. Lett. **61**, 1658 (1988).
[10]H. A. Blackstead, Phys. Rev. B **47**, 11 411 (1993); Physica C **209**, 437 (1993).
[11]J. C. Phillips, Phys. Rev. B **42**, 8623 (1990); **43**, 11 415 (1991).
[12]K. M. Rabe, J. C. Phillips, P. Villars, and I. D. Brown, Phys. Rev. B **45**, 7650 (1992).
[13]W. K. Kwok *et al.*, Phys. Rev. Lett. **67**, 390 (1991).
[14]J. C. Phillips, Phys. Rev. **104**, 1263 (1956).
[15]R. P. Sharma, F. J. Rotella, J. D. Jorgensen, and L. E. Rehn, Physica C **174**, 409 (1991); L. C. Feldman, J. W. Mayer, and S. T. Icraux, *Materials Analysis by Ion Channeling* (Academic, New York, 1982), Chap. IV.
[16]J. C. Phillips, Phys Rev. B **47**, 11 615 (1993); G. A. Thomas *et al.*, *ibid.* **46**, 1553 (1992); L. S. Martinson, J. W. Schweitzer, and N. C. Baenziger, Phys. Rev. Lett. **71**, 125 (1993).
[17]M. Gazda *et al.*, Physica C **207**, 300 (1993).
[18]G. Rietveld, N. Y. Chen, and D. van der Marel, Phys. Rev. Lett. **69**, 2578 (1992). The mathematical models discussed in this paper to explain the discontinuity in $d\mu/dT$ at $T=T_c$ are simplistic. The discontinuity is simply the signature of the onset of spinodal phase separation. The mathematical models assume that the surface is two-dimensional, whereas it is actually $(2+1)$-dimensional. Also at the transition in a two-dimensional homogeneous metal there will always be Kosterlitz-Thouless fluctuations which eliminate any discontinuities in $d\mu/dT$ which are obtained in simplistic models.
[19]R. Griessen *et al.*, Phys. Rev. Lett. **72**, 1910 (1994).
[20]J. C. Phillips, Phys. Rev. Lett. **72**, 3863 (1994).
[21]C. Kawabata, S. R. Shenog, and A. R. Bishop (unpublished).